



Published in final edited form as:

Radiat Res. 2021 January 01; 195(1): 93–100. doi:10.1667/RADE-20-00063.1.

CIRP Sensitizes Cancer Cell Responses to Ionizing Radiation

Weichao Sun^{a,e}, Adele P. Bergmeier^{a,b}, Yi Liao^{a,f}, Shiyong Wu^{a,c,d}, Lingying Tong^{a,c,1}

^aEdison Biotechnology Institute, Ohio University, Athens, Ohio 45701

^bDepartment of Biological Sciences and Ohio University, Ohio 45701

^cDepartment of Chemistry and Biochemistry and Ohio University, Ohio 45701

^dProgram of Molecular and Cellular Biology, Ohio University, Ohio 45701

^eThe First Affiliated Hospital of Shenzhen University, Shenzhen Second People's Hospital, Shenzhen, China

^fDepartment of Thoracic Surgery, Southwest Hospital, Army Medical University (Third Military Medical University), Chongqing, China

Abstract

Cold inducible RNA binding protein (CIRP), also named A18 hnRNP or CIRBP, is a cold-shock RNA-binding protein which can be induced upon various cellular stresses. Its expression level is induced in various cancer tissues relative to adjacent normal tissues; this is believed to play a critical role in cancer development and progression. In this study, we investigated the role of CIRP in cells exposed to ionizing radiation. Our data show that CIRP reduction causes cell colony formation and cell viability reduction after irradiation. In addition, CIRP knockdown cells demonstrated a higher DNA damage rate but less cell cycle arrest after irradiation. As a result, the induced DNA damage with less DNA repair processes led to an increased cell apoptosis rate in CIRP knockdown cells postirradiation. These findings suggest that CIRP is a critical protein in irradiated cells and can be used as a potential target for sensitizing cancer cells to radiation therapy.

INTRODUCTION

Cold-inducible RNA binding protein (CIRP), also known as A18 hnRNP or CIRBP, is a member of the cold-shock protein family (1). This stress-induced protein responds to various cellular stresses, including hypoxia (2), hypothermal stress (3) and ultraviolet (UV) radiation (4, 5). Our previously reported study revealed that CIRP can only be induced using low-dose UVB radiation, but not high-dose UVB radiation, in human keratinocytes. After repeated low-dose UVB irradiation, CIRP is involved in transforming normal keratinocytes to cancerous cells, which implicates the activation of both NF- κ B and Stat3 pro-survival pathways (6). In addition, CIRP helps the primary cells to avoid replicative senescence and thus become cancerous cells (7). The expression level of CIRP has been proved to be higher

¹Address for correspondence: Edison Biotechnology Institute, 101 Konneker Laboratories, The Ridges, Building 25, Athens, OH 45701; tongl1@ohio.edu.

in cancer cells compared to adjacent normal tissues in cancer patients; this is believed to be related to its pro-survival signaling (8).

Radiation therapy is a widely accepted treatment for human cancers; with approximately one half of all newly diagnosed patients receiving radiotherapy during the course of cancer treatment (9, 10). However, high-dose therapeutic radiation can cause severe health problems due to the radiation-induced damage to adjacent normal tissues, and may cause early onset of cytokine cascades (11, 12). Cancer cells that survive irradiation may become senescent and recur later in the patient's lifespan (13). Thus, understanding the cellular mechanisms which respond and promote cell survival is critical to improving the efficacy of radiation therapy. CIRP is involved in cell survival pathways and closely linked to cancer development and progression, there is reason to believe that CIRP facilitates cancer cell survival in radiation therapy. Therefore, CIRP could be used as a target to increase cancer cell sensitivity to radiation therapy.

In this study, we investigated the role of CIRP in cancer cells treated with radiation. Our data indicate that CIRP regulates cellular responses to radiation and may serve as a target for radiosensitizer development.

MATERIALS AND METHODS

Cell Culture

Human melanoma cells A375 and M624 were grown in DMEM (Gibco®, Grand Island, NY) supplemented with 10% fetal bovine serum (FBS; Gibco) and 1% Penicillin-Streptomycin (HyClone™ Laboratories, Logan, UT). All cells were incubated at 37°C with 5% CO₂.

CIRP Knockdown Stable Cell Line Establishment

The gRNA sequence of CIRP was inserted into a PX330 vector (Addgene, Cambridge, MA). The PX330-CIRP vector was co-transfected with a pLenti-CMV-GFP-puro vector at a 5:1 ratio into A375 and M624 cells. After 72 h of transfection, puromycin (1 µg/ml) was added for selection. After one week, cells were seeded into 96-well cell culture plates, one cell per well. CIRP expression level was detected using Western blot and cell colonies with reduced CIRP expression were selected and used for further experiments.

Cell Proliferation Assay

Cell proliferation was determined using an MTT based toxicology assay kit (Sigma-Aldrich® LLC, St. Louis, MO). A375, A375^{CIRP^{-/-}}, M624 and M624^{CIRP^{-/-}} cells were seeded onto 6-well plates at a density of 1×10^5 cells/well and incubated overnight for proper attachment. Cells were then either sham irradiated or exposed to 2 Gy. At a designated time, 24, 48 or 72 h postirradiation, MTT solution (10× dilution) was added into the wells for a 3-h incubation. Absorbance at 570 nm was measured using a Cytation™ 3 Cell Imaging Reader (BioTekt® Instruments Inc., Winooski, VT).

Clonogenic Assay

A375, A375^{CIRP^{-/-}}, M624 and M624^{CIRP^{-/-}} cells were seeded into plates at the density of 800 cells/60-mm dish, and incubated for attachment overnight. Cells were then either sham irradiated or exposed to 2 Gy. After 5–7 days of incubation, the cells were fixed with cold methanol for 10 min at –20°C and stained with 1% crystal violet in 25% methanol for 10 min at room temperature. Fixed cells were then rinsed with water, and colonies with a size greater than 0.4 mm were counted using Kodak Molecular Imaging Station *In Vivo* F system (Eastman Kodak, Rochester, NY).

Cell Cycle Analysis

A375 and A375^{CIRP^{-/-}} cells were seeded in 60-mm tissue culture dish and starved in FBS-free media for 24 h to synchronize the cell cycle. The FBS-free media was then replaced with full media and cells were irradiated at 0, 2, 5 or 10 Gy. At 24 h postirradiation, the cells were harvested in pellet form by Trypsin and washed twice with ice-cold phosphate buffered saline (PBS). Cells were then fixed in 70% ice-cold ethanol for at least 30 min at 4°C, followed by two washes in PBS. RNase, 50 µl (100 µg/ml), and 200 µl PI (50 µg/ml) were added to the fixed cells to degrade RNA and to stain DNA. Stained cells were analyzed using an Accuri™ C6 flow cytometer (BD Biosciences, Franklin Lakes, NJ).

Western Blot Analysis

Cells were lysed with Nonidet™ P-40 (NP-40) lysis buffer (2% NP-40, 80 mM NaCl, 100 mM Tris-HCl pH 8.0, 0.1% SDS) with proteinase inhibitor mixture (cOmplete™, Roche Diagnostics, Indianapolis, IN). Cell lysates were incubated on ice for 15 min and then centrifuged at 16,000g at 4°C for 15 min. Protein concentration was measured using the Protein DC Assay Kit (Bio-Rad® Laboratories Inc., Hercules, CA). Equal amounts of protein were subjected to SDS-PAGE and transferred to nitrocellulose membrane. The membranes were then blocked in 5% milk in Tris-buffered saline plus Tween® 20 (TBST) for 45 min and probed with anti-CIRP, anti-γ-H2AX and anti-PARP (all acquired from Cell Signaling Technology® Inc., Danvers, MA) or anti-β-actin (Santa Cruz Biotechnology® Inc., Dallas, TX) at 4°C overnight. After rinsing with TBST, the membrane was incubated with corresponding HRP-conjugated anti-rabbit or anti-mouse anti-body for 45 min at room temperature. Membranes were then washed three times in TBST followed by 2× wash in Tris-buffered saline (TBS), and developed in SuperSignal™ West Pico chemiluminescent substrate (Pierce™ Biotechnology, Rockford, IL). The images were captured and analyzed using the Odyssey® Imager equipped with Odyssey Image Studio software (LI-COR® Inc., Lincoln, NE). Band intensity was quantitated using ImageJ software (National Institutes of Health, Bethesda, MD).

Statistical Analysis

Data are expressed as the mean ± SD with each experiment repeated at least three times. The statistical significance of differences for the mean values between groups was determined using Student's *t* test. Differences with *P* < 0.05 were considered statistically significant.

RESULTS

Knockdown CIRP Sensitizes Cancer Cells to Ionizing Radiation

The growth rate of the melanoma cells was first determined using clonogenic assays to compare A375, A375^{CIRP^{-/-}} cells, and M624, M624^{CIRP^{-/-}} cells with or without irradiation. The results showed that the colony number was reduced by approximately 50% in A375 cells after 2 Gy irradiation. A375^{CIRP^{-/-}} cells had approximately 35% of colonies formed compared to A375 cells. Irradiation (2 Gy) of A375^{CIRP^{-/-}} further reduced the colony numbers to 10% compared to nonirradiated A375 cells (Fig. 1A and B). Similar results were observed in M624 cells, where radiation reduced colony numbers to 80% of the nonirradiated M624 cells, and CIRP knockdown resulted in approximately 50% reduction. Irradiated M624^{CIRP^{-/-}} cells showed reduced colony numbers to approximately 20% (Fig. 1C and D). The knockdown of CIRP in both cell lines was confirmed by Western blot showing >70% reduction in CIRP protein expression in cells (Fig. 1E). The data indicate that CIRP plays a pro-proliferative role in both melanoma cell lines, and a synergetic effect in both cell lines when CIRP knockdown cells are exposed to radiation.

The rate of short-term (within 72 h after seeding) cell proliferation was also determined in melanoma cells compared to CIRP knockout cells. In A375 cells, the cell numbers increased to approximately 3.5-fold in 72 h without treatment and to 2.5-fold in CIRP knockdown cells. The 3.5-fold induction reduced to 2.4-fold in irradiated A375 cells, and 2.5-fold induction reduced to 1.5-fold in irradiated A375^{CIRP^{-/-}} cells at 72 h (Fig. 2A). In M624 cells, nonirradiated cell numbers increased to 4.5-fold in 72 h, and CIRP knockdown reduced the induction to approximately threefold. After irradiation, the cell number of M624 cells increased to 1.3-, 2.7- and 3.1-fold after 24, 48 and 72 h, respectively. Additionally, M624^{CIRP^{-/-}} cells increased to 1.2- and 2.1-fold after 24 and 48 h, and remained at 1.9-fold at 72 h (Fig. 2B).

CIRP Regulates Cell Cycle after Irradiation

We further measured the role of CIRP in regulating cell cycles after irradiation. A375 and A375^{CIRP^{-/-}} cells were irradiated to 0, 2, 5 and 10 Gy, and cell cycles were analyzed 24 h after irradiation. Radiation doses of 0, 2 and 5 Gy did not cause significant cell cycle arrest in A375 and A375^{CIRP^{-/-}} cells. However, after 10 Gy irradiation of A375 cells, G₂/M phase increased from 26% to 43%, while G₀/G₁ phase reduced from 54% to 42% and S phase reduced from 19% to 9% in 24 h. In A375^{CIRP^{-/-}} cells, no significant change could be detected in G₂/M or G₀/G₁ phases, while the S phase reduced slightly from 18% to 14%. These data indicate that CIRP may facilitate cells passing the cell cycle check point in radiation-induced cell cycle arrest (Fig. 3).

CIRP Affects Radiation-Induced DNA Damage

Since the progression of cell cycle is responsive to DNA damage and DNA repair progress, we determined the DNA damage level in A375 and A375^{CIRP^{-/-}} cells after irradiation. The expression level of γ -H2AX in cells was used as a DNA damage marker. In A375 cells, the c-H2AX expression level was induced to 2.1-fold in 15 min and 3.2-fold in 2 h, but reduced to background level at 4 h after 2 Gy irradiation. After 5 Gy irradiation, γ -H2AX

was induced to 3.5-fold in 15 min and reduced to approximately 1.5-fold in 2 and 4 h. In A375^{CIRP^{-/-}} cells, γ -H2AX was induced to 6.1-fold at 2 and 4 h postirradiation, with no significant change at 15 min postirradiation. In 5 Gy irradiated A375^{CIRP^{-/-}} cells, γ -H2AX expression level was induced to 12-, 10- and 15-fold at 15 min, 2 h and 4 h, respectively. The data showed that A375 cells demonstrated DNA repair progress at 2 and 4 h, while no DNA repair was observed in A375^{CIRP^{-/-}} cells (Fig. 4).

CIRP is Critical in Regulating Cell Apoptosis—Since the DNA damage level was not reduced after irradiation in A375^{CIRP^{-/-}} cells, and minimal cell cycle arrest was observed, we next investigated the cell apoptosis status of A375 and A375^{CIRP^{-/-}} cells. The Western blot of cleaved PARP showed that a 2 Gy dose caused an approximately 3.5-fold induction in cleaved PARP in A375 cells, and >7-fold induction in A375^{CIRP^{-/-}} cells. This indicated a lack of DNA repair progress, cell cycle arrest in CIRP knockdown cells, and an increased apoptosis rate after irradiation (Fig. 5).

DISCUSSION

CIRP is known to be activated by stressors, and its activation usually facilitates cell survival (3, 14). CIRP also inhibits DNA damage-induced apoptosis and affects chemotherapeutic sensitivity in cancer cells (15, 16). Our previously report study showed that CIRP regulates Stat3 and NF- κ B pathways, which both promote cell survival after UVB irradiation (6, 17, 18). However, the activation of these pro-survival signaling pathways often leads to cancer cell recovery after radiation treatment. In this report, we investigated the role of CIRP in cancer cell proliferation after irradiation. Knockdown CIRP in A375 cells decreases the cell viability and growth rate. This effect is synergistic to the effect of radiation on inhibiting the cancer cell proliferation (Figs. 1 and 2). These data confirm previously reported findings that CIRP is a pro-survival protein and helps the cells to survive under stress (16, 19). As radiation is known to induce cell cycle arrest, which relates closely to cell proliferation, we next determined the effect of CIRP on cell cycle arrest after irradiation. However, the radiation-induced cell cycle arrest was eliminated in CIRP knockdown cells, parental cancer cells were arrested after irradiation at G₀/G₁ phase, which is consistent with previously published studies (Fig. 3) (20–22). In addition, the level of γ -H2AX constantly increased in a dose- and time-dependent manner in CIRP knockdown cells within 4 h postirradiation, while the level of γ -H2AX increased but then began to decrease at 4 h in parental cells after irradiation. It is possible that the accumulation of DNA damage and non-arrested cell cycle after irradiation is the reason for lower cell viability and cell growth rate. We concur with the previously reported study that knockdown CIRP leads to more DNA damage in irradiated cells, although we had contrary data in γ -H2AX expression, as previously published work showed that the level of γ -H2AX increased more than parental cells in the first 10 min postirradiation and then decreased within 60 min compared to parental cancer cells (23). The different pattern of γ -H2AX may be due to cell line difference, since the DNA repair system in various cell lines may be different (24). In addition, the level of γ -H2AX is more commonly accepted as a DNA damage marker rather than DNA repair marker, especially in human skin cells (25–28). We further showed that unrepaired DNA damage and unregulated cell cycle lead to the higher level of apoptosis, as indicated by the induction of cleaved

PARP protein (Fig. 5). To conclude, we demonstrated that CIRP is a critical pro-cell survival and proliferation gene, which also participates in repairing DNA damage after irradiation. CIRP could be a potential target to sensitize the cancer cells to radiotherapy.

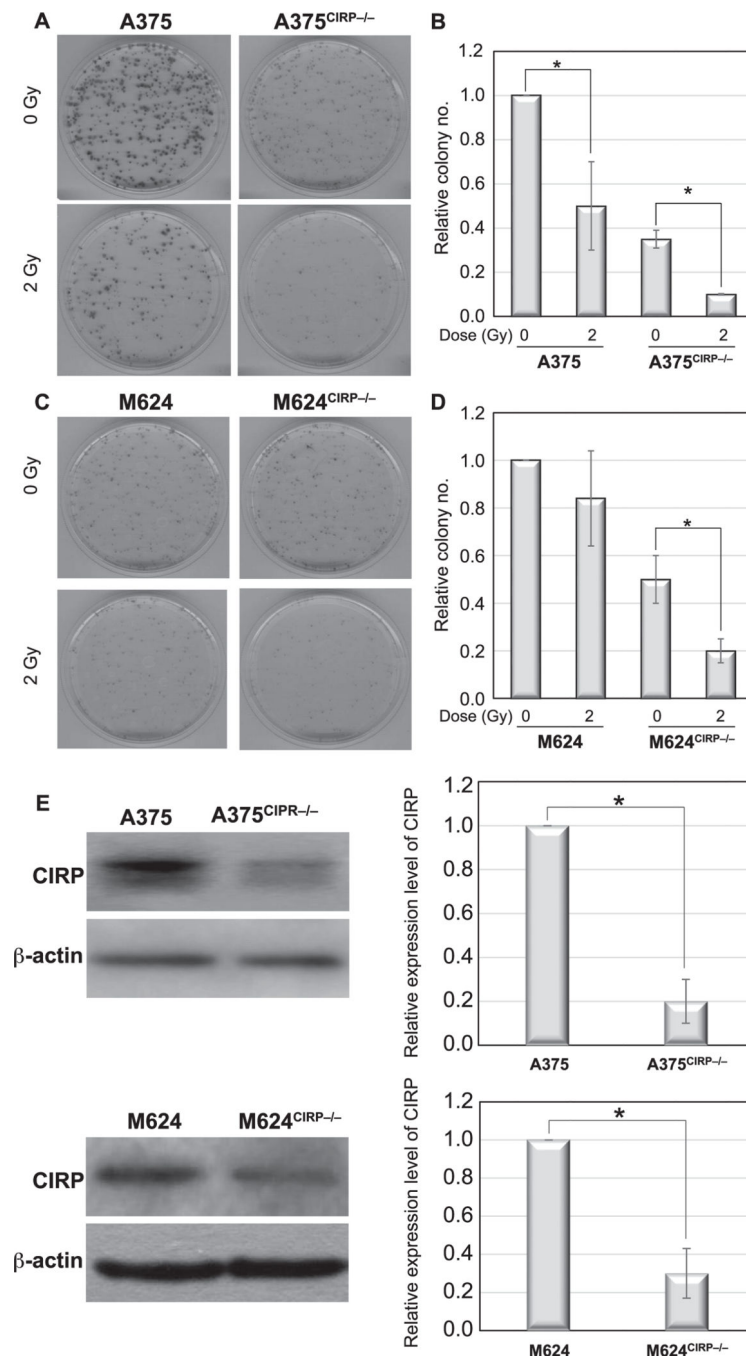
ACKNOWLEDGMENTS

This work was partially supported by American Cancer Society Postdoctoral Fellowship PF-1605101-NEC (to LT), research start-up funds from Edison Biotechnology Institute at Ohio University (to LT) and the National Institutes of Health [grant no. R01 1R01ES030425-01A1 (to SW)].

REFERENCES

1. Nishiyama H, Itoh K, Kaneko Y, Kishishita M, Yoshida O, Fujita J. A glycine-rich RNA-binding protein mediating cold-inducible suppression of mammalian cell growth. *J Cell Biol* 1997; 137:899–908. [PubMed: 9151692]
2. Wellmann S, Buhner C, Moderegger E, Zelmer A, Kirschner R, Koehne P, et al. Oxygen-regulated expression of the RNA-binding proteins RBM3 and CIRP by a HIF-1-independent mechanism. *J Cell Sci* 2004; 117:1785–94. [PubMed: 15075239]
3. Zhu X, Buhner C, Wellmann S. Cold-inducible proteins CIRP and RBM3, a unique couple with activities far beyond the cold. *Cell Mol Life Sci* 2016; 73:3839–59. [PubMed: 27147467]
4. Sheikh MS, Carrier F, Papathanasiou MA, Hollander MC, Zhan Q, Yu K, et al. Identification of several human homologs of hamster DNA damage-inducible transcripts. Cloning and characterization of a novel UV-inducible cDNA that codes for a putative RNA-binding protein. *J Biol Chem* 1997; 272:26720–6.
5. Yang C, Carrier F. The UV-inducible RNA-binding protein A18(A18 hnRNP) plays a protective role in the genotoxic stress response. *J Biol Chem* 2001; 276:47277–84.
6. Sun W, Liao Y, Yi Q, Wu S, Tang L, Tong L. The mechanism of CIRP in regulation of STAT3 phosphorylation and Bag-1/S expression upon UVB radiation. *Photochem Photobiol* 2018; 94:1234–39. [PubMed: 29981150]
7. Artero-Castro A, Callejas FB, Castellvi J, Kondoh H, Carnero A, Fernandez-Marcos PJ, et al. Cold-inducible RNA-binding protein bypasses replicative senescence in primary cells through extracellular signal-regulated kinase 1 and 2 activation. *Mol Cell Biol* 2009; 29:1855–68. [PubMed: 19158277]
8. Ren WH, Zhang LM, Liu HQ, Gao L, Chen C, Qiang C, et al. Protein overexpression of CIRP and TLR4 in oral squamous cell carcinoma: an immunohistochemical and clinical correlation analysis. *Med Oncol* 2014; 31:120. [PubMed: 25027624]
9. Baskar R, Lee KA, Yeo R, Yeoh KW. Cancer and radiation therapy: current advances and future directions. *Int J Med Sci* 2012; 9:193–9. [PubMed: 22408567]
10. Ringborg U, Bergqvist D, Brorsson B, Cavallin-Stahl E, Ceberg J, Einhorn N, et al. The Swedish Council on Technology Assessment in Health Care (SBU) systematic overview of radiotherapy for cancer including a prospective survey of radiotherapy practice in Sweden 2001–summary and conclusions. *Acta Oncol* 2003; 42:357–65. [PubMed: 14596499]
11. Bentzen SM. Preventing or reducing late side effects of radiation therapy: radiobiology meets molecular pathology. *Nat Rev Cancer* 2006; 6:702–13. [PubMed: 16929324]
12. Donnelly EH, Nemhauser JB, Smith JM, Kazzi ZN, Farfan EB, Chang AS, et al. Acute radiation syndrome: assessment and management. *South Med J* 2010; 103:541–6. [PubMed: 20710137]
13. Moding EJ, Kastan MB, Kirsch DG. Strategies for optimizing the response of cancer and normal tissues to radiation. *Nat Rev Drug Discov* 2013; 12:526–42. [PubMed: 23812271]
14. Lujan DA, Ochoa JL, Hartley RS. Cold-inducible RNA binding protein in cancer and inflammation. *Wiley Interdiscip Rev RNA* 2018; 9.
15. Lee HN, Ahn SM, Jang HH. Cold-inducible RNA-binding protein, CIRP, inhibits DNA damage-induced apoptosis by regulating p53. *Biochem Biophys Res Comm* 2015; 464:916–21. [PubMed: 26188505]

16. Zhou KW, Jiang K, Zhu W, Weng G. Expression of cold-inducible RNA-binding protein (CIRP) in renal cell carcinoma and the effect of CIRP downregulation cell proliferation and chemosensitivity to gemcitabine. *Oncol Lett* 2018; 15:7611–16. [PubMed: 29849797]
17. Liao CK, Jeng CJ, Wang HS, Wang SH, Wu JC. Lipopolysaccharide induces degradation of connexin43 in rat astrocytes via the ubiquitin-proteasome proteolytic pathway. *PLoS One* 2013; 8:e79350.
18. Liao Y, Tong L, Tang L, Wu S. The role of cold-inducible RNA-binding protein in cell stress response. *Int J Cancer* 2017; 141:2164–73. [PubMed: 28608439]
19. Zhong P, Huang H. Recent progress in the research of cold-inducible RNA-binding protein. *Future Sci OA* 2017; 3:FSO246.
20. Reed MF, Liu VF, Ladha MH, Ando K, Griffin JD, Weaver DT, et al. Enforced CDK4 expression in a hematopoietic cell line confers resistance to the G1 arrest induced by ionizing radiation. *Oncogene* 1998; 17:2961–71. [PubMed: 9881698]
21. Teyssier F, Bay JO, Dionet C, Verrelle P. Cell cycle regulation after exposure to ionizing radiation. (Article in French). *Bull Cancer* 1999; 86:345–57. [PubMed: 10341340]
22. McIlwrath AJ, Vasey PA, Ross GM, Brown R. Cell cycle arrests and radiosensitivity of human tumor cell lines: dependence on wild-type p53 for radiosensitivity. *Cancer Res* 1994; 54:3718–22. [PubMed: 8033090]
23. Chen JK, Lin WL, Chen Z, Liu HW. PARP-1-dependent recruitment of cold-inducible RNA-binding protein promotes double-strand break repair and genome stability. *Proc Natl Acad Sci U S A* 2018; 115:E1759–E68.
24. Sedelnikova OA, Bonner WM. GammaH2AX in cancer cells: a potential biomarker for cancer diagnostics, prediction and recurrence. *Cell Cycle* 2006; 5:2909–13. [PubMed: 17172873]
25. Sharma A, Singh K, Almasan A. Histone H2AX phosphorylation: a marker for DNA damage. *Methods Mol Biol* 2012; 920:613–26.
26. Mah LJ, El-Osta A, Karagiannis TC. gammaH2AX: a sensitive molecular marker of DNA damage and repair. *Leukemia* 2010; 24:679–86. [PubMed: 20130602]
27. Barnes L, Dumas M, Juan M, Noblesse E, Tesniere A, Schnebert S, et al. GammaH2AX, an accurate marker that analyzes UV genotoxic effects on human keratinocytes and on human skin. *Photochem Photobiol* 2010; 86:933–41. [PubMed: 20492564]
28. Warters RL, Adamson PJ, Pond CD, Leachman SA. Melanoma cells express elevated levels of phosphorylated histone H2AX foci. *J Invest Dermatol* 2005; 124:807–17. [PubMed: 15816840]

**FIG. 1.**

The role of CIRP in cell viability after irradiation. CIRP knockdown cells were established in A375 and M624 cell lines. Clonogenic assays of A375, A375^{CIRP-/-} and M624, M624^{CIRP-/-} cells after sham irradiation or 2 Gy irradiation were performed. Panel A: Representative plates of A375 and A375^{CIRP-/-} cells. Panel B: Quantitative analysis of the number of A375 and A375^{CIRP-/-} cell colonies. Panel C: Representative plates of M624 and M624^{CIRP-/-} cells. Panel D: Quantitative analysis of the number of M624 and M624^{CIRP-/-} cells. Panel E: Western blots of CIRP and β-actin in A375 and A375^{CIRP-/-} cells. Panel F: Relative expression level of CIRP in A375 and A375^{CIRP-/-} cells. Panel G: Western blots of CIRP and β-actin in M624 and M624^{CIRP-/-} cells. Panel H: Relative expression level of CIRP in M624 and M624^{CIRP-/-} cells.

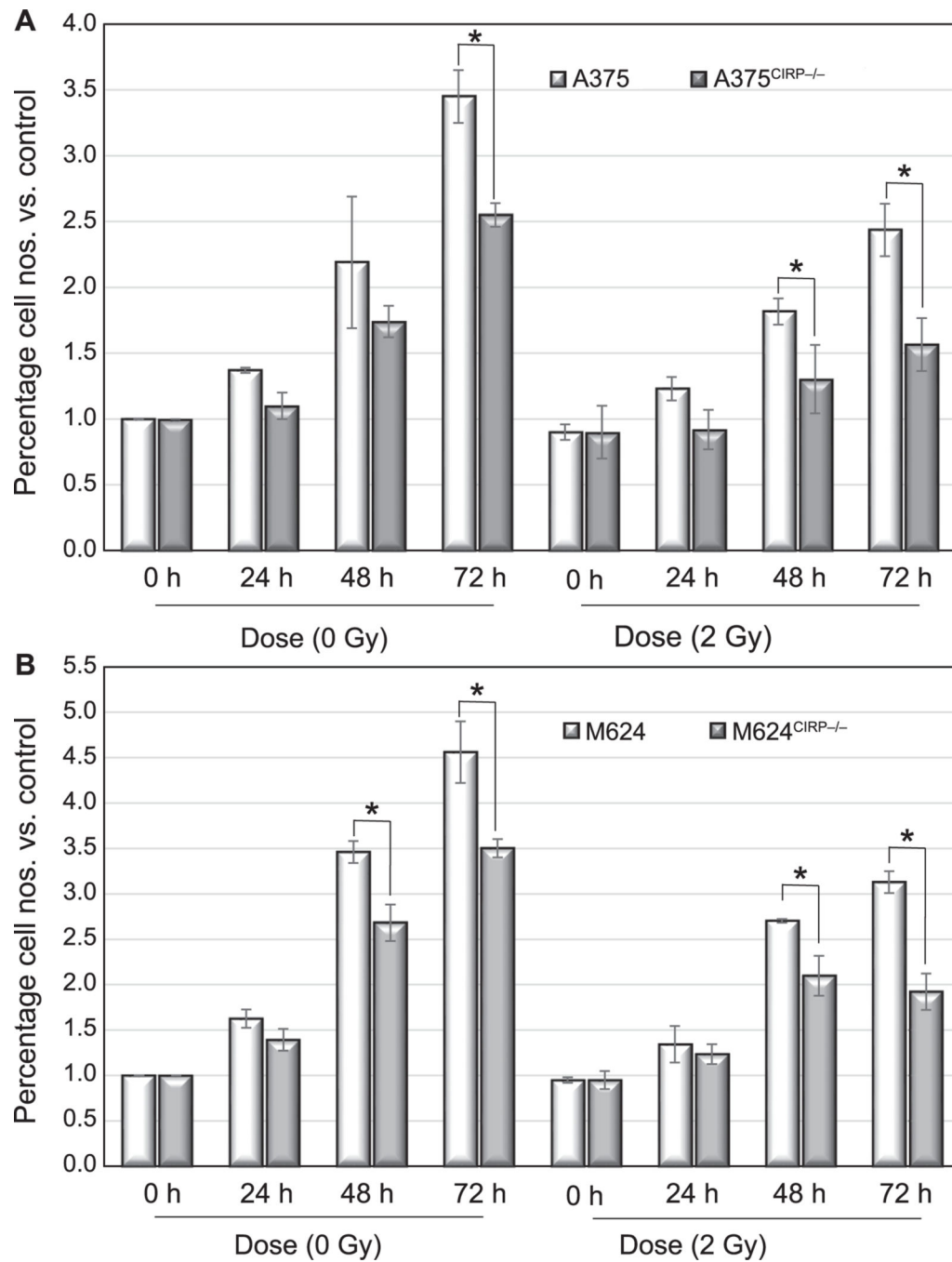
cell colonies. Panel E: Confirmation of CIRP knockdown in both A375 and M624 cells using Western blot and quantitative analysis. * $P < 0.05$ compared to control group.

Author Manuscript

Author Manuscript

Author Manuscript

Author Manuscript

**FIG. 2.**

The role of CIRP in cell viability after irradiation. MTT assay was performed to determine cell viability for (panel A) A375 and (panel B) M624 cells after sham irradiation or 2 Gy irradiation at 0, 24, 48 and 72 h. * $P < 0.05$ compared to control group.

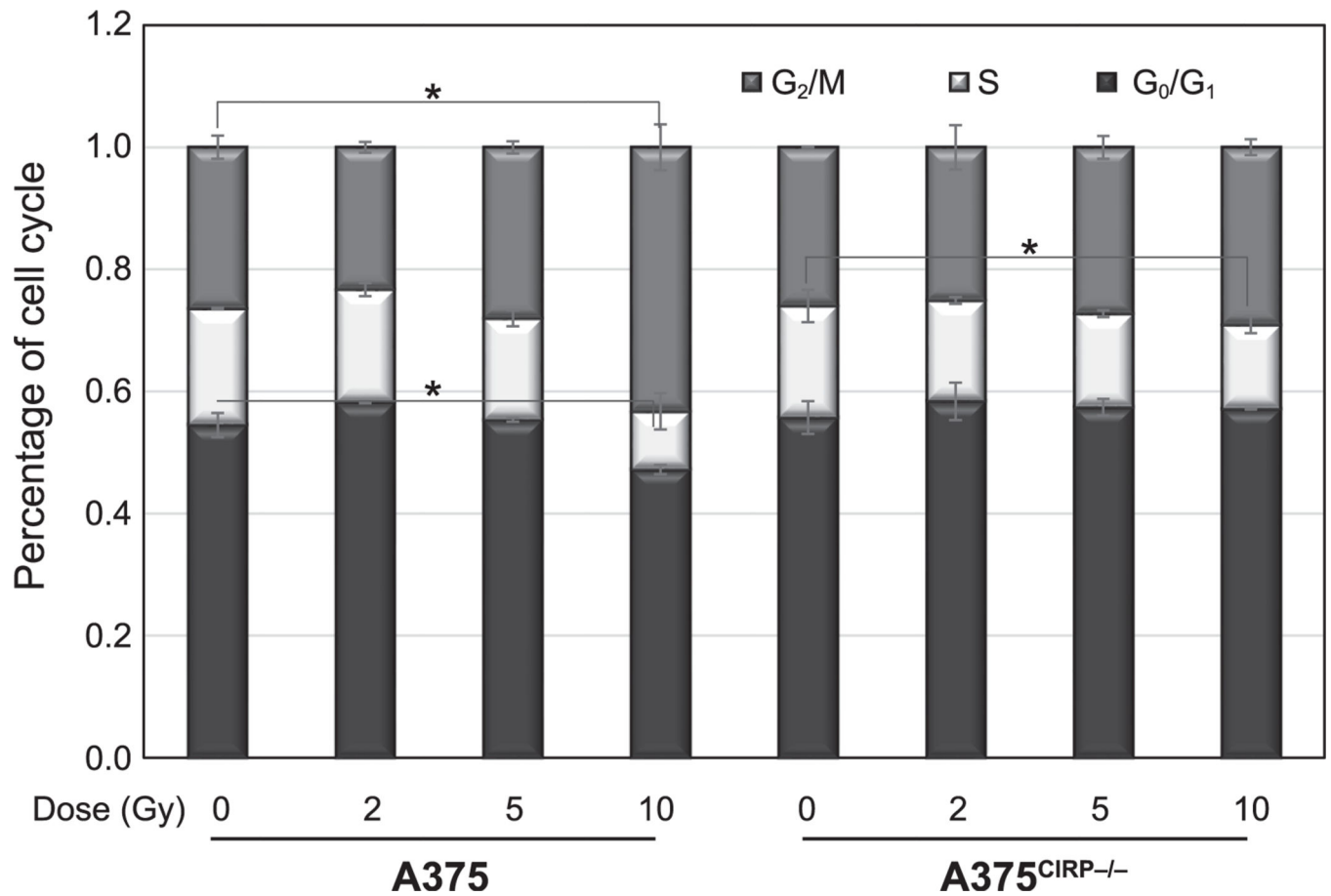
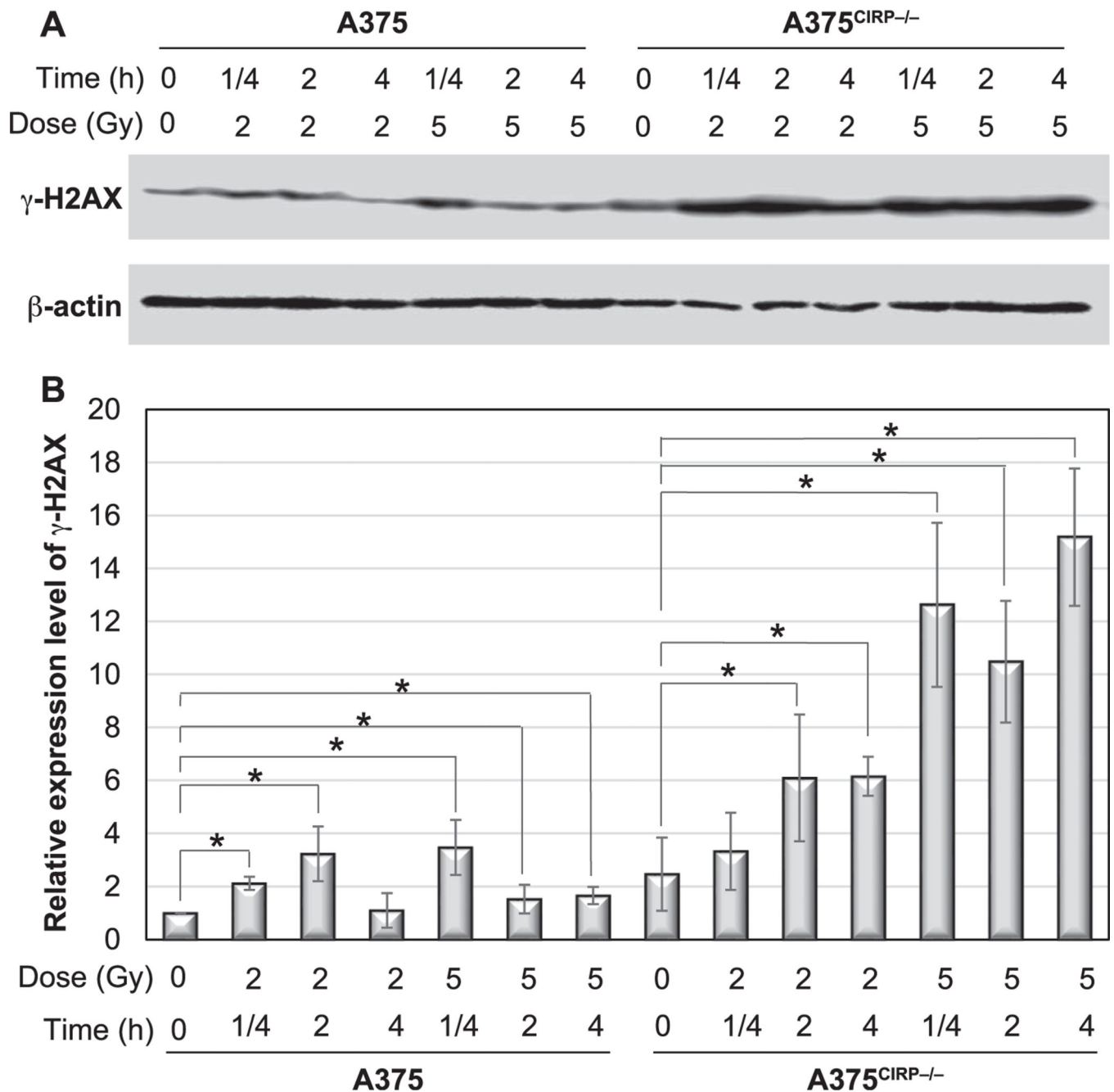


FIG. 3. CIRP regulates cell cycles after irradiation. A375 and A375^{CIRP-/-} cells were synchronized in FBS-free media for 24 h and then received 0, 2, 5 or 10 Gy. Full media was added into cells immediately after irradiation. Cell cycle analysis was performed at 24 h postirradiation using flow cytometry. * $P < 0.05$ compared to control group.

**FIG. 4.**

The level of γ -H2AX in cells after irradiation. A375 and A375^{CIRP-/-} cells were irradiated at 0, 2 and 5 Gy and proteins were extracted at the indicated time points postirradiation. The protein level of γ -H2AX was determined using Western blot analysis (panel A) and band intensity was quantitated using ImageJ software (panel B). * $P < 0.05$ compared to control group.

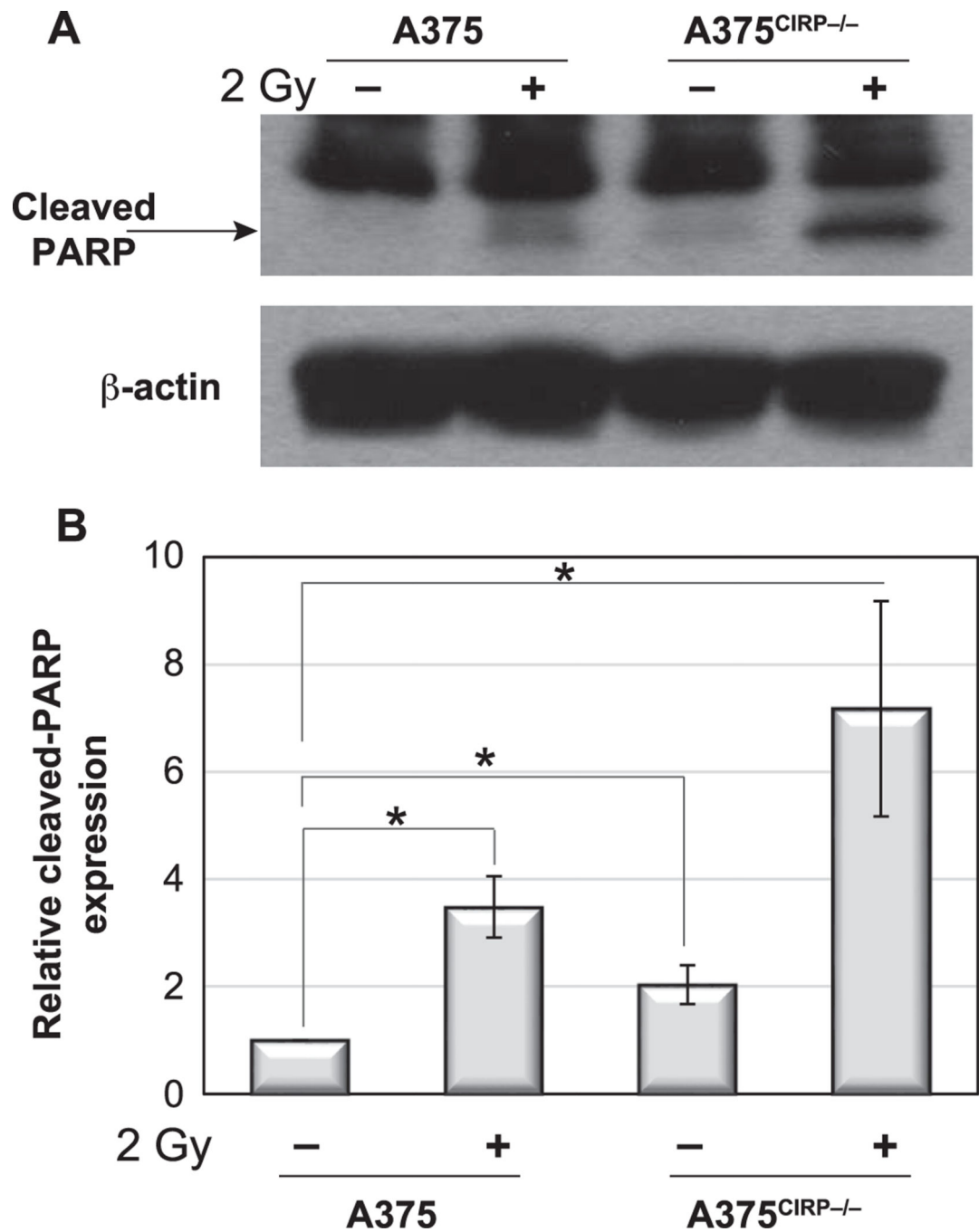


FIG. 5. Role of CIRP in regulating PARP cleavage. The cleaved PARP in A375 and A375^{CIRP-/-} cells at 24 h with or without 2 Gy irradiation was determined using Western blot analysis (panel A) and band intensity was quantitated using ImageJ software (panel B). * $P < 0.05$ compared to control group.